

MEASUREMENT OF INSERTION LOSS OF AN ACOUSTIC TREATMENT IN THE PRESENCE OF ADDITIONAL UNCORRELATED SOUND SOURCES

Jacob Klos* and Daniel L. Palumbo*
Structural Acoustics Branch
NASA Langley Research Center
Hampton, Virginia 23681

A method to intended for measurement of the insertion loss of an acoustic treatment applied to an aircraft fuselage *in-situ* is documented in this paper. Using this method, the performance of a treatment applied to a limited portion of an aircraft fuselage can be assessed even though the untreated fuselage also radiates into the cabin, corrupting the intensity measurement. This corrupting noise in the intensity measurement incoherent with the panel vibration of interest is removed by correlating the intensity to reference transducers such as accelerometers. Insertion loss of the acoustic treatments is estimated from the ratio of correlated intensity measurements with and without a treatment applied. In the case of turbulent boundary layer excitation of the fuselage, this technique can be used to assess the performance of noise control methods without requiring treatment of the entire fuselage. Several experimental studies and numerical simulations have been conducted, and results from three case studies are documented in this paper. Conclusions are drawn about the use of this method to study aircraft sidewall treatments.

Introduction

In aircraft, a major cause of interior noise is turbulent boundary layer pressure fluctuations outside the aircraft that transmit sound through the fuselage. Acoustical treatments are typically attached to the fuselage to abate this noise transmitted into the aircraft interior. Thus, it is desirable to quantify the acoustical performance of these noise control methods to select the most effective. However, the treatments are typically assessed in a laboratory environment or by predictive methods, not in flight conditions. To measure the performance of an acoustic treatment in flight, extraneous acoustic sources must not corrupt an intensity measurement in the vicinity of the treated section. This requires that a large portion of the fuselage be treated or a small test section must be acoustically isolated from the untreated fuselage. Both of these options are costly and time consuming. It is desirable to measure the acoustical performance of treatments applied to a small area of the fuselage during flight to assure laboratory and operational characteristics agree. Consequently, experimental methods to measure and compare different acoustical treatments applied to a limited portion of the fuselage *in-situ* are needed.

An experimental method to measure the insertion loss of an acoustic treatment using intensity measurements made in the presence of corrupting sound is proposed in this paper. The method is based on coherence techniques that are used to decompose a sound field into partial sound fields that are correlated with the response of a specific sound source.¹⁻⁶ Alfredson¹ used

these techniques to study the sound produced by components of a diesel engine. The responses of microphones surrounding a diesel engine were correlated to a microphone placed in the far field. The area of the engine that contributed most significantly to the response of a far field microphone was identified. The benefits and limitations of the method were argued. It was discussed that good correlation between two signals does not necessarily indicate a causal relationship. This is especially true for tonal components of a sound field. It was discussed that coherence techniques are most applicable to broadband sources, and not easily applied to tonal sources. Wang² applied partial coherence techniques to the problem of source identification. The sound radiated by three speakers excited with both mutually incoherent and partially coherent signals were studied. Again, the problem of a coherent versus causal relationship was discussed. Recently, Takata et. al.³ and Kwon et. al.^{4,5} have applied partial coherence techniques to near-field acoustical holography to extract the partial sound field correlated with reference signals. These measurements were used to assess the sound caused by components of a motor vehicle power train.^{3,4} Pilkinton et. al.⁶ used partial coherence techniques to determine the sound pressure level at a microphone location caused by one source in the presence of a second, incoherent source. Good agreement between expected and calculated sound pressure levels were obtained with the partial coherence method. The current effort extends these works by using partial coherence methods to resolve the intensity radiated by a sound source in the presence of additional, uncorrelated sound sources for the purpose of assessing the effectiveness of an acoustic treatment.

In the case of turbulent boundary layer induced noise inside aircraft, the correlation lengths of the excitation

* Aerospace Engineer, Structural Acoustics Branch
This material is declared a work of the U.S. Government and is not subject to copyright protection in the United States.

pressure field are small relative to the size of the fuselage and the excitation spectrum is broadband in nature.⁷ Thus, distant points on the fuselage can be approximated as independent, incoherent vibratory sources that radiate into the aircraft interior. Therefore, as long as the dimensions of the acoustic treatment are large in comparison to the turbulent boundary layer correlation length, the noise resulting from an untreated and a treated portion of the fuselage can be considered incoherent. The sound produced by the untreated areas of the fuselage can be rejected from intensity measurements near the treated area by correlating the intensity measurement to the fuselage vibration in the treated area. Thus, the insertion loss of a particular treatment can be found from correlated intensity measurements with and without the treatment applied to the fuselage.

Formulation for a Single Reference Transducer

Acoustic intensity is commonly measured using a two-microphone acoustic intensity probe by methods documented in the literature.⁸ Assuming simple harmonic behavior and a stationary process, the acoustic intensity parallel to the axis of the probe is

$$I = \frac{1}{2\omega\Delta x} \text{IM}[G_{xy}] \quad (1)$$

where ω is angular frequency, Δx is the microphone separation distance, and G_{xy} is the cross spectrum of the two microphone signals⁹

$$G_{xy} = X^* Y \quad (2)$$

where X and Y are the discrete Fourier transforms of the pressure time histories of microphone one and microphone two respectively and $*$ indicates the conjugation of a complex number. The correlated intensity is calculated using a reference transducer z . Assuming simple harmonic behavior and a linear and stationary process, the transfer function between each of the microphones, x and y , and the reference transducer, z , are⁹

$$H_{zx} = \frac{XZ^*}{ZZ^*} \quad (3)$$

and

$$H_{zy} = \frac{YZ^*}{ZZ^*} \quad (4)$$

where Z is the Fourier transform of the time history of the reference transducer. The transfer functions shown in equations (3) and (4) are calculated using an H1 estimate. Calculation of a transfer function using the H1 estimate rejects noise uncorrelated to the reference signal, in this case the reference transducer z . The power spectrum of the reference transducer is

$$G_{zz} = Z^* Z \quad (5)$$

The correlated cross spectrum, in which the noise incoherent to the reference transducer has been rejected,

is reconstructed from the transfer functions and the power spectrum

$$G_{xy,z} = H_{zx}^* H_{zy} G_{zz} \quad (6)$$

The correlated intensity is

$$I_c = \frac{1}{2\omega\Delta x} \text{IM}[G_{xy,z}] \quad (7)$$

This approach is similar to one that has been proposed by Marroquin.¹⁰ To distinguish between the different intensity calculations, intensity calculated using equation (1) is termed uncorrelated intensity and intensity calculated using equation (7) is termed correlated intensity. This terminology will be used in the discussion of experimental results.

Formulation for Multiple Reference Transducers

The formulation of the correlated intensity using a single reference transducer can be expanded to multiple references. To compute the intensity correlated to a set of reference transducers, a set of linearly independent transfer functions between the reference transducers and the responses of the intensity probe microphones is needed. Using the methods for the calculation of ordered, conditioned transfer functions, reference⁹ specifically pgs. 226-238, the intensity incoherent with several reference transducers can be rejected from an intensity measurement. A brief review of the essential theory in matrix form is given here; however, intricacies of the calculations and fundamental concepts are left to Bendat.⁹ Let q be the total number of reference transducers, and $q+1$ be a response transducer of interest. The elements in the conditioned cross spectral matrix, $[G]$, are found from the recursion relation

$$G_{i,j,r} = G_{i,j,(r-1)} - \frac{G_{r,j,(r-1)} G_{i,r,(r-1)}}{G_{r,r,(r-1)}} \quad (8)$$

where the conditioned cross spectral matrix $[G]$ is a three dimensional $(q+1)$ by $(q+1)$ by q matrix and the indices corresponding to a specific transducer. The indices are ordered in the following way

$$i = 1, 2, 3, \dots, q+1 \quad (9a)$$

$$j = 1, 2, 3, \dots, q+1 \quad (9b)$$

$$r = 1, 2, 3, \dots, q \quad (9c)$$

The response transducer must be ordered as the $(q+1)^{\text{th}}$ transducer corresponding to the $(q+1)^{\text{th}}$ elements in $[G]$. For example, the first set of entries in the matrix are computed for the case when $r=1$ as

$$G_{i,j,1} = G_{ij} - \frac{G_{1j} G_{i1}}{G_{11}} \quad (10)$$

for $i = 1, 2, 3, \dots, q+1$ and $j = 1, 2, 3, \dots, q+1$. When $i \neq j$ in equation (10), G_{ij} is the measured cross spectrum between transducers i and j , G_{1j} is the measured cross spectrum between transducers 1 and j , G_{i1} is the measured power spectrum of transducer 1 , and G_{11} is

the measured cross spectrum between transducers i and l . When $i=j$ in equation (10), $G_{ij} = G_{ii}$ is the measured power spectrum if transducer i , $G_{lj} = G_{li}$ is the measured cross spectrum between transducers l and i , G_{ll} is the measured power spectrum of transducer l , and G_{il} is the measured cross spectrum between transducers i and l . From equation (8), the second entries in the conditioned cross spectral matrix, when $r=2$, are computed from the first set of entries in the matrix

$$G_{i,j,2} = G_{i,j,1} - \frac{G_{2,j,1}G_{i,2,1}}{G_{2,2,1}} \quad (11)$$

where all of the terms on the right hand side of equation (11) are found from equation (10). The third set of entries in the conditioned cross spectral matrix, when $r=3$, are

$$G_{i,j,3} = G_{i,j,2} - \frac{G_{3,j,2}G_{i,3,2}}{G_{3,3,2}} \quad (12)$$

where all of the terms on the right hand side of equation (12) are found from equation (11). The remaining elements in $[G]$, for $r=4$ and so on, are found from the recursion relation given by equation (8) following the pattern shown in equations (10), (11) and (12). The ordered, conditioned H1 transfer function estimate between reference transducer r and response transducer $q+1$ are found from the elements in the conditioned cross spectral matrix

$$L_{r(q+1)} = \frac{G_{r,(q+1),(r-1)}}{G_{r,r,(r-1)}} \quad (13)$$

where the indices of G correspond to the elements in the three dimensional conditioned cross spectral matrix $[G]$. Consider an example where a measurement consists of four reference transducers and one response transducer. Then $[G]$ would be a 5 by 5 by 4 matrix computed using equations (8) through (12). The ordered, conditioned transfer function between reference transducer 3 and response transducer 5 is

$$L_{35} = \frac{G_{3,5,2}}{G_{3,3,2}} \quad (14)$$

It should be noted that each element in the conditioned cross spectral matrix, $[G]$, is frequency dependent.

Intensity measurements are made with a common two-microphone acoustic intensity probe. Let x be the first microphone and y be the second microphone of the intensity probe which are simultaneously sampled along with q reference transducers. The ordered, conditioned transfer functions between the reference transducers and the first microphone, L_{rx} for $r=1, 2, \dots, q$, are computed for the case when the $q+1$ response transducer is the first microphone x . The ordered, conditioned transfer functions between the reference transducers and the second microphone, L_{ry} for $r=1, 2, \dots, q$, are computed for the case when the $q+1$ response transducer is the second microphone y . The cross

spectrum of the microphones x and y of the intensity probe, conditioned by the q reference transducers, is

$$G_{xy,q} = \sum_{r=1}^q L_{rx}^* L_{ry} G_{r,r,(r-1)} \quad (15)$$

where $*$ indicates the conjugation of a complex number, $G_{r,r,(r-1)}$ are elements in the cross spectral matrix corresponding to the power spectrum of transducer r , and the L are found from equation (10). The conditioned intensity is

$$I_q = \frac{1}{2\omega\Delta x} IM[G_{xy,q}] \quad (16)$$

where ω is angular frequency, Δx is the microphone separation distance, and $G_{xy,q}$ is the conditioned cross spectrum of the two microphone signals. The summation used to calculate the conditioned cross spectrum between the microphones in equation (15) is based on the H1 transfer function estimate of the reference transducers input to the microphones output. Thus, the noise in the cross spectrum between the two microphones incoherent to the reference transducers is rejected in the calculation of $G_{xy,q}$. The intensity calculated using equation (16) is the portion of the measured intensity that is coherent to the set of reference transducers. The intensity in the measurement incoherent to the set of reference transducers is rejected. To distinguish between the different intensity calculations, intensity calculated using equation (16) is termed conditioned intensity in the remaining sections of the paper. With $q=1$, this formulation for multiple reference transducers exactly reduces to the formulation for a single reference transducer given by equations (3) through (7).

The formulation for multiple reference transducers can also be used to reject intensity correlated to one subset of reference transducers while accepting intensity from a second subset of reference transducers. The set of q reference transducers is divided into two subsets, where the intensity correlated to N reference transducers is rejected and the intensity correlated to $q-N$ reference transducers is accepted. The indices in $[G]$ are ordered in the following way

$$i = 1, 2, \dots, N, N+1, \dots, q+1 \quad (17a)$$

$$j = 1, 2, \dots, N, N+1, \dots, q+1 \quad (17b)$$

$$r = 1, 2, \dots, N, N+1, \dots, q \quad (17c)$$

which correspond to specific reference transducers. The first 1 through N transducers must be selected as the transducers to which the correlated intensity will be rejected. Then the calculation of the cross spectrum is

$$G_{xy,q} = \sum_{r=N+1}^q L_{rx}^* L_{ry} G_{r,r,(r-1)} \quad (18)$$

and the intensity is found from equation (16). Thus, the intensity correlated only to the $N+1$ through q reference transducers is accepted, while the intensity correlated to the 1 through N transducers as well as the intensity uncorrelated to any reference transducer is rejected. This formulation can be useful when trying to reject a known sound source from an intensity measurement.

Experimental Implementation

Measurements of the correlated intensity are made using a narrow band FFT analyzer. The analyzer is used to measure the cross spectra between the intensity probe microphones and the reference transducers and the power spectra of all of the transducers. These spectra are used to calculate the uncorrelated, correlated and conditioned intensity as outlined above. The capability to reject noise in an intensity measurement uncorrelated to a set of reference transducers has been found to be highly dependant on the experimental setup and the sampling parameters. Since these dependencies could comprise a paper of their own, only a brief review of the significant findings will be documented here.

The level of uncorrelated noise which can be rejected using the methods outlined above is dependant on the number of ensemble averages used to calculate the cross spectrum between the various transducers and the number of reference transducers. The noise rejection level, in dB, that can be rejected from the measured intensity is

$$NRL = 10 \log_{10} \left[\left(\frac{1}{N-q+1} \right)^{1/2} \right] \quad (19)$$

where N is the number of averages used to compute the cross spectrum, and q is the number of reference transducers used to compute the correlated or conditioned intensity. For example, to reject up to 20 dB of intensity that is uncorrelated to 100 reference transducers, at least 10,099 averages must be taken. The metric given by equation (19) yields a reliability estimate when the correlated intensity method is used. When the level of measured intensity rejected by the proposed methods approaches this level, the measurement should be treated with caution.

Measurements of the acoustic energy flow through a measurement surface are typically of interest and are found from the surface integral of the normal intensity. The methods documented above require that the transfer function between the reference transducers and the intensity probe microphones be linear and stationary. This requirement, in part, demands that the intensity normal to the measurement surface be sampled at discrete points in space, averaged, and multiplied by the area of the surface to estimate the

energy flow. The common method of estimating energy flow using a continuous, moving sweep of an intensity probe over a measurement surface cannot be used as it violates the requirement of stationary transfer functions.

Case Study 1

The first case study is an idealized representation of the problem of interest, designed to test the basic experimental approach. Two speakers were placed 6-feet apart in an anechoic room and a two-microphone acoustic intensity probe was placed halfway between the two speakers (Figure 1). The speakers were driven with mutually uncorrelated white noise. The level at which speaker 1 was excited was kept constant throughout the test. The excitation level of speaker 2 was varied to produce different levels of sound uncorrelated to the sound produced by speaker 1 and the intensity was measured at the probe position. Measurement of the intensity radiated by speaker 1 at the probe position in the presence of the corrupting sound produced by speaker 2 was desired. The responses of the microphones were measured, as was the excitation signal to speaker 1. The auto spectra and cross spectra between each of the transducers were calculated from an ensemble average of ten thousand frames. No overlap and a boxcar window were used. The uncorrelated intensity was calculated using equation (1) from the cross spectrum of the intensity probe microphones. The correlated intensity was calculated using equation (7) from the cross spectra of the intensity probe microphones with the excitation signal to speaker 1 as a reference. These two methods of calculating the intensity at the probe were compared for various excitation levels of speaker 2.

The results of this case study are shown in Figure 2. Results are illustrated for speaker 2 excited at four different levels while the excitation level of speaker 1 is held constant. The sound pressure level at the acoustic intensity probe is about 35 dB when speaker 1 is excited and speaker 2 is off (Figure 2a, \bullet - line). As the excitation level of speaker 2 is turned on and increased to its highest value, the sound pressure level at the microphone increases to 65 dB (Figure 2a, \times - line). The uncorrelated intensity is shown in Figure 2b. The intensity radiated by speaker 1 at the probe location is illustrated by the case when speaker 2 is off (Figure 2b, \bullet - line). The uncorrelated intensity calculated from equation (1) is corrupted when speaker 2 is excited (Figure 2b, all lines except the \bullet - line) and the intensity level radiated by speaker 1 cannot be determined using equation (1). The correlated intensity calculated using the excitation to speaker 1 as a reference is shown in Figure 2c. The correlated intensity calculated using equation (7) is nearly

independent of the excitation level of speaker 2. The portion of the measured intensity radiated by speaker 2 is rejected and the intensity level of speaker 1 is recovered. This case study demonstrates the capability of the method to reject intensity uncorrelated to a known source.

Case Study 2

The second case study was designed to demonstrate the measurement of the insertion loss of an acoustic treatment in the presence of corrupting noise. The insertion loss of lead vinyl applied to a curved honeycomb composite panel was found in the presence of corrupting noise. The experimental setup used in this study is illustrated in Figures 3 through 5. A curved honeycomb composite panel was installed in the transmission loss window in the Structural Acoustic Loads and Transmission (SALT) facility (Figure 3) at NASA Langley Research Center.¹¹ The SALT facility is a transmission loss suite consisting of a reverberation room and anechoic room connected by a 54-inch by 54-inch transmission loss window. The reverberation room was excited, using speakers, by broadband random noise to produce a diffuse acoustic excitation of the panel (Figure 5a). To increase the mass of the panel, limp lead vinyl was applied using double-sided tape (Figure 4). A baseline measurement of the insertion loss of the lead vinyl was found by measuring the sound power radiated by the panel using acoustic intensity methods.¹² A traverse mechanism (Figure 5c) was used to scan 4 acoustic intensity probes across a measurement surface located 10-cm in front of the panel.¹² The insertion loss of the lead vinyl was computed as the ratio of the radiated sound power with and without the lead vinyl attached keeping the excitation of the reverberation room constant (Figure 4). The insertion loss of the lead vinyl from 800 to 5000 Hz is shown in Figure 6 (blue line).

Next, the anechoic room was excited by speakers placed approximately 10 feet from the transmission loss window (Figure 5b) to simulate uncorrelated noise in the aircraft interior. The speakers in the anechoic room were driven by broadband noise that was uncorrelated to the simultaneous excitation of the reverberation room. The intensity radiated from the panel was measured in the presence of the uncorrelated excitation of the anechoic room. The intensity, computed using equation (1), was sampled at 272 discrete locations on the measurement surface. The auto and cross spectra were computed from 1000 averages taken at a sampling frequency of 12,800 Hz with a frame length of 2048 points. The radiated sound power was computed from the measured intensity. The uncorrelated insertion loss was computed from the ratio of the radiated sound power measured with and without the lead vinyl

attached to the panel. The uncorrelated insertion loss of the lead vinyl for the case of an excitation of reverberation room and an uncorrelated excitation of the anechoic room is shown in Figure 6 (red line).

Finally, the intensity measurements that were made in the presence of the uncorrelated excitation of the anechoic room were correlated using equation (7) to an accelerometer mounted on the panel at a random location (Figure 5d). Since there were only two uncorrelated sources, it was found that only one accelerometer was needed to capture the energy correlated to the reverberant excitation. The correlated sound power radiated from the panel was computed from the correlated intensity. The correlated insertion loss was computed from the ratio of the correlated sound power with and without the lead vinyl applied to the panel. The correlated insertion loss of the lead vinyl for an excitation of reverberation room and an uncorrelated excitation of the anechoic room is shown in Figure 6 (green line).

When noise is added to the anechoic room and the intensity measurements are not correlated to the panel vibration (Figure 6, red line), the estimated insertion loss of the lead vinyl is not in good agreement with the baseline measurement (Figure 6, blue line). When noise is added to the anechoic room and the intensity measurements are correlated to the panel vibration (Figure 6, green line), the estimated insertion loss of the lead vinyl is in good agreement with the baseline measurement (Figure 6, blue line). Thus, the correlation method can be used to measure the insertion loss of acoustic treatments in the presence of an uncorrelated noise source.

Case Study 3

The third case study was designed to demonstrate the ability to assess the insertion loss of an acoustic treatment applied to a panel excited by flow. Sound radiated from a fuselage panel mounted in the test section of the Structural Acoustic Flow Apparatus (SAFA) wind tunnel at NASA Langley Research Center was studied (Figure 7a). The fuselage panel was a rib stiffened aluminum panel typical of aircraft construction (Figure 7b). The skin was 0.063-inches thick and each of the six 10-inches by 20-inches bays were separated by aluminum stiffeners. The panel was pre-strained to simulate the effects of pressurization present during flight. Sixteen accelerometers were mounted on four of the six the bays (Figure 7c and 8). The tunnel was operated at a flow speed of 160 ft/sec, which resulted in a substantial turbulent boundary layer excitation of the panel causing sound to be radiated from each of the bays. Intensity measurements in front of bays one and two were correlated to the

accelerometers on these bays to assess the performance of an acoustic treatment applied to the fuselage panel. The intensity measurements were made using four intensity probes mounted to a traverse mechanism (Figure 7d). The acoustic intensity radiated from bays one and two was sampled at 32 discrete points in front of the bays using the four intensity probes. To provide acoustic isolation from the surrounding environment, the acoustic intensity probes were placed in an anechoic enclosure that was butted up against the test section of the wind tunnel (Figure 7d). All six bays radiate into the anechoic enclosure.

The insertion loss of trim panels applied to the fuselage panel was assessed. The trim panels were 0.020-inch thick aluminum panels that were attached to the stiffeners of the fuselage panel. There was a 3-inch air gap between the fuselage panel and the trim panels. The acoustic intensity radiated from bays one and two for 3 treatment cases were measured

- Case 1: No treatment applied bays (Figure 9a)
- Case 2: Treatment applied all bays (Figure 9b)
- Case 3: Only bays 1 and 2 treated (Figure 9c)

The intensity at each of the 32 measurement points was calculated using the uncorrelated intensity method equation (1), the correlated intensity method equation (7), and the conditioned intensity method equation (16). In the case of the correlated intensity calculation, accelerometer 9 was used as a reference. In the case of the conditioned intensity calculation, all of the accelerometers on bays 1, 2, 3, and 4 were used as references. The intensity correlated to the subset of accelerometers on bays 1 and 2 was accepted while the intensity correlated to the subset of accelerometers on bays 3 and 4 was rejected using equation (18). Two thousand averages were taken at a sampling frequency of 12,800 Hz with a frame length of 1024 points. No overlap and a boxcar window were used. The uncorrelated, correlated and conditioned energy flows were computed from the intensity. The energy flow through the measurement surface in front of bays one and two was found by averaging the 32 discrete intensity measurements and multiplying by the area of the measurement surface. The insertion loss of an acoustic treatment applied to the fuselage panel was found from the ratio of the energy flow through the measurement surface with and without the treatment in place. The turbulent boundary layer excitation magnitude was assumed to remain constant.

The baseline insertion loss of the trim panel was found from the ratio of the uncorrelated energy flow of treatment Case 1 and treatment Case 2. This baseline provides an accurate estimate of the insertion loss since the sound radiated from all 6 bays was reduced by the same magnitude. The baseline insertion loss is shown

in Figure 10a-c, ~~—~~ line. To assess the proposed methods, the insertion loss of the trim panel was computed from the energy flows of treatment Case 1 and treatment Case 3 using the uncorrelated, correlated and conditioned intensity calculations and was compared to the baseline insertion loss. This comparison is shown in Figure 10a-c.

There is poor agreement between the baseline insertion loss and the insertion loss measured when only bays 1 and 2 are treated and the intensity is found using the uncorrelated calculation (Figure 10a). Untreated bays 3, 4, 5 and 6 radiate into the anechoic enclosure and corrupt the uncorrelated intensity measurement in front of bays one and two resulting in an under-estimate of the insertion loss. There is significantly better agreement between the baseline insertion loss and the insertion loss measurement when only bays 1 and 2 are treated and the intensity is computed using the correlated intensity calculation (Figure 10b) and the conditioned intensity calculation (Figure 10c). When the intensity is correlated to reference accelerometers placed on the panel in the treated area, the intensity radiated by bays 3, 4, 5 and 6 is rejected, and the insertion loss can be measured.

Conclusions

A method to measure intensity radiated by a sound source in the presence of uncorrelated sound has been presented and experimentally verified. Three case studies were presented illustrating the usefulness of the method for studying aircraft interior acoustics. The results obtained in the presence of uncorrelated sound with the correlated and conditioned intensity methods were in good agreement with results obtained with traditional intensity measurements made in the absence of uncorrelated sound. The insertion loss of an acoustic treatment can be assessed by rejecting noise radiated by sources that are uncorrelated to the fuselage vibration in the treated area. This method will provide a useful tool for the *in-situ* study and diagnostics of noise control treatments applied to an aircraft fuselage.

References

1. Alfredson, R. J., 1977, "The partial coherence technique for source identification on a diesel engine," *Journal of Sound and Vibration*, **55**(4), pp. 487-494.
2. Wang, M. E., and M. J. Crocker, 1983, "On the application of coherence techniques for source identification in a multiple noise source environment," *Journal of the Acoustical Society of America*, **74**(3), pp. 861-872.
3. Takata, H., T. Nishi, W. Jiang and J. S. Bolton, 1996, "The use of near-field acoustical holography (NAH) and partial-field decomposition to identify

and quantify the sources of exterior noise radiated from a vehicle,” *Journal of the Acoustical Society of America*, **100**(4), pp. 2654-2655.

4. Kwon, H., J. S. Bolton and J. K. Hammond, 1997, “A comparison of partial coherence and singular value partial field decomposition in the context of near-field acoustical holography,” *Journal of the Acoustical Society of America*, **102**(5), p. 3076.
5. Kwon, H., and J. S. Bolton, 1998, “Partial field decomposition in near-field acoustical holography by the use of singular value decomposition and partial coherence procedures”, *Proceedings of Noise-Con 98*, Ypsilanti, Michigan.
6. Pilkinton, G. D., W. E. Simmons and W. F. Wenneman, 1998, “Source quantification using partial coherence in a controlled experiment”, *Proceedings of Noise-Con 98*, Ypsilanti, Michigan.
7. Mathur, G. P., B. N. Tran and M. A. Simpson, 1999, “MD-90 cabin noise diagnostics ground and flight tests”, *AIAA Conference Paper*, #AIAA-99-1834.
8. Fahy, F., 1995, *Sound Intensity*. London: E & F N Spon.
9. Bendat, J. S., and A. G. Piersol, 1986, *Random Data: Analysis and Measurement Procedures*. New York: John Wiley & Sons.
10. Marroquin, M., 2001, “New innovation in sound intensity: selective intensity”, *Proceedings of SAE NVH Conference*, Traverse City, MI.
11. Grosveld, F., 1999, “Calibration of the Structural Acoustic Loads and Transmission (SALT) facility at NASA Langley Research Center,” *Proceedings of Inter-noise 99*, Fort Lauderdale, Florida.
12. Klos, J., and S. A. Brown, 2002, “Automated transmission loss measurement in the Structural Acoustic Loads and Transmission facility at NASA Langley Research Center,” *Proceedings of Inter-noise 2002*, Detroit, MI.

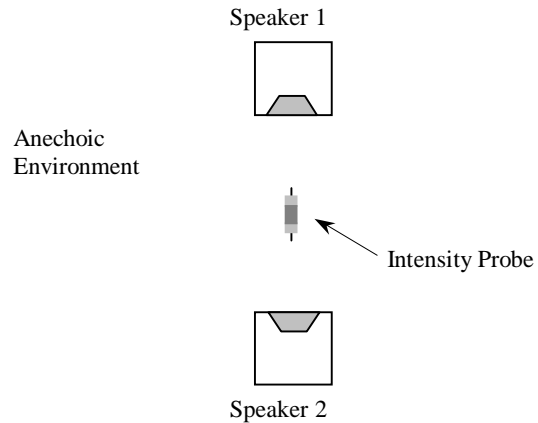
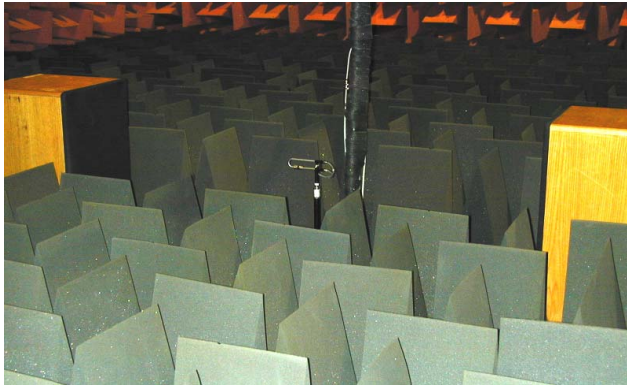


Figure 1: Speaker setup for the investigation of correlated intensity measurements.

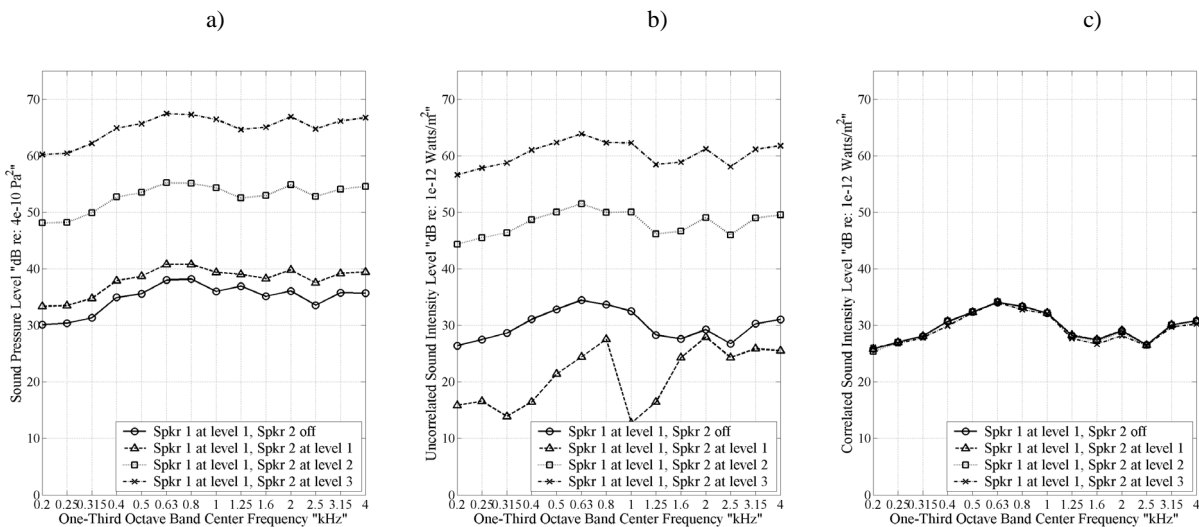


Figure 2: Results with the speakers in the 180° configuration: a) sound pressure level at one of the intensity probe microphones, b) uncorrelated intensity level at the intensity probe and c) correlated intensity level.

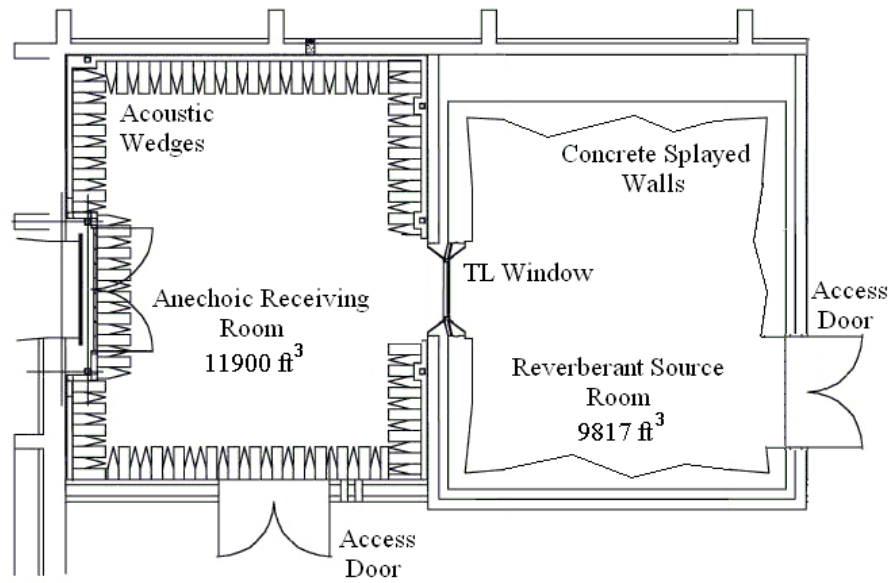


Figure 3: Structural acoustic loads and transmission facility.

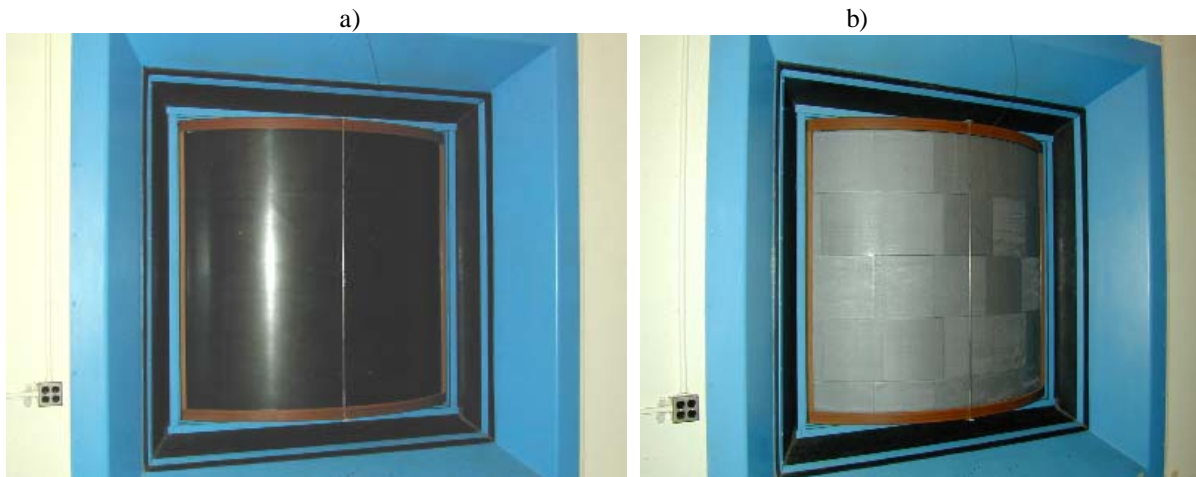


Figure 4: View of the composite panel from the reverberation room: a) the composite panel mounted in the transmission loss window and b) the composite panel with lead vinyl attached to the surface. The insertion loss of the lead vinyl is measured by exciting the reverberation room and measuring the sound power radiated into the anechoic room.

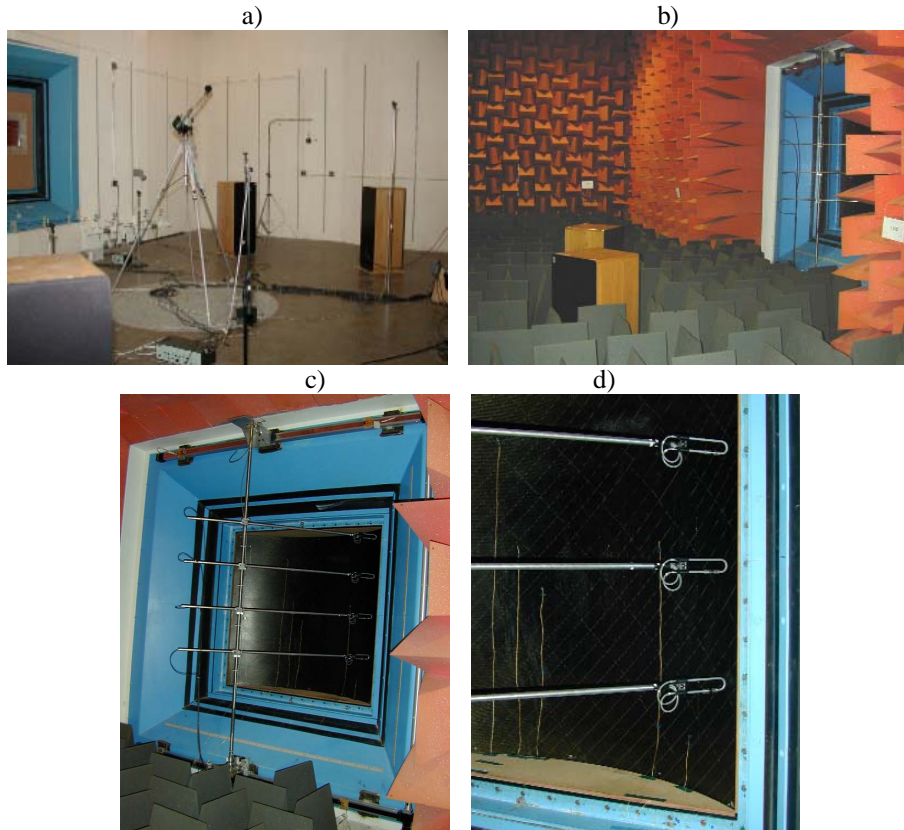


Figure 5: Case study 2 experimental setup: a) excitation of the reverberation room by four speaker (only three are pictured) which simulates excitation of the aircraft exterior, b) speakers used to excite the anechoic room which simulates uncorrelated noise in the aircraft interior, c) setup used to scan the intensity radiated from the panel and d) accelerometers are mounted to the panel and used as a reference signal for the correlation method.

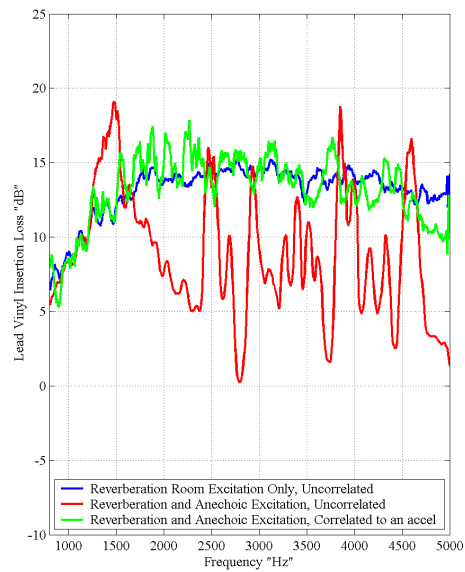


Figure 6: Insertion loss of the lead vinyl.

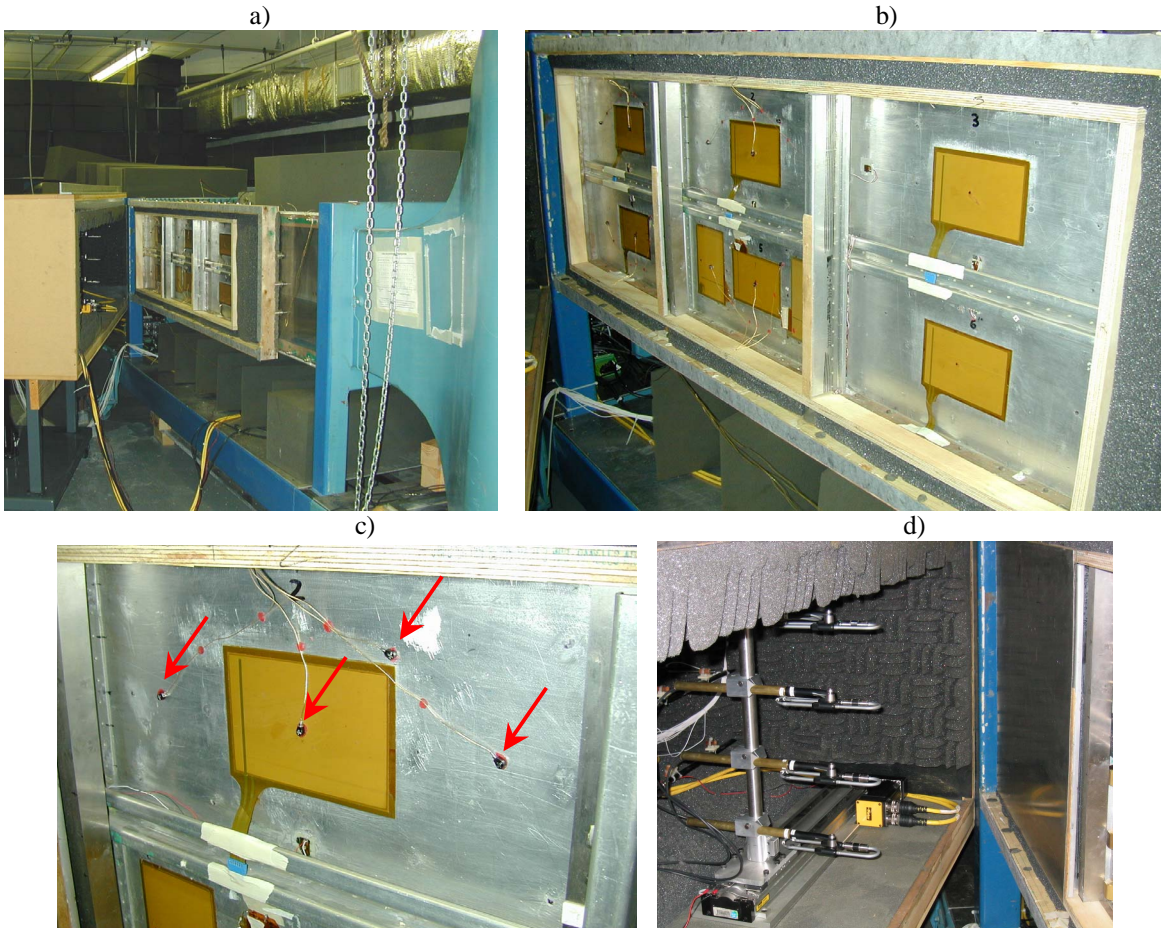


Figure 7: Case study 3 experimental setup: a) wind tunnel test section with the fuselage panel mounted, b) close up of the fuselage panel showing the six bays, c) accelerometers mounted to one of the bays as indicated by the arrows and d) intensity probes in the anechoic box.

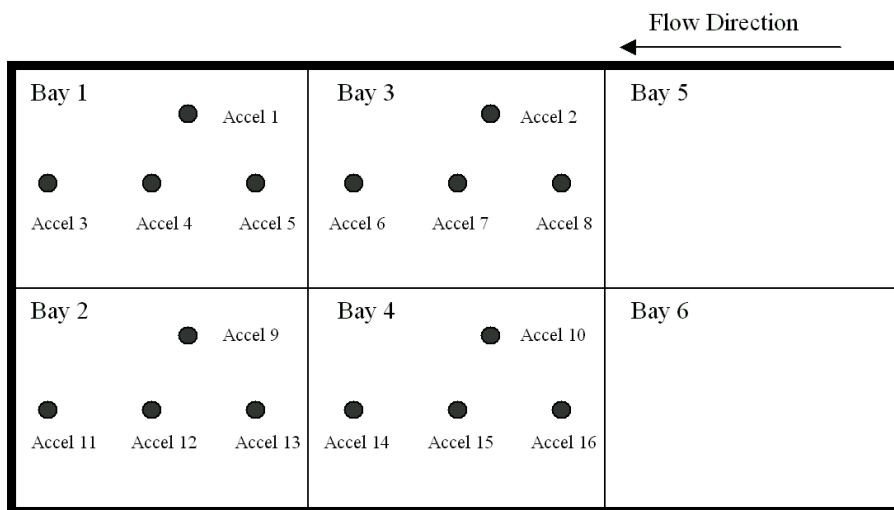


Figure 8: Schematic of the bays.

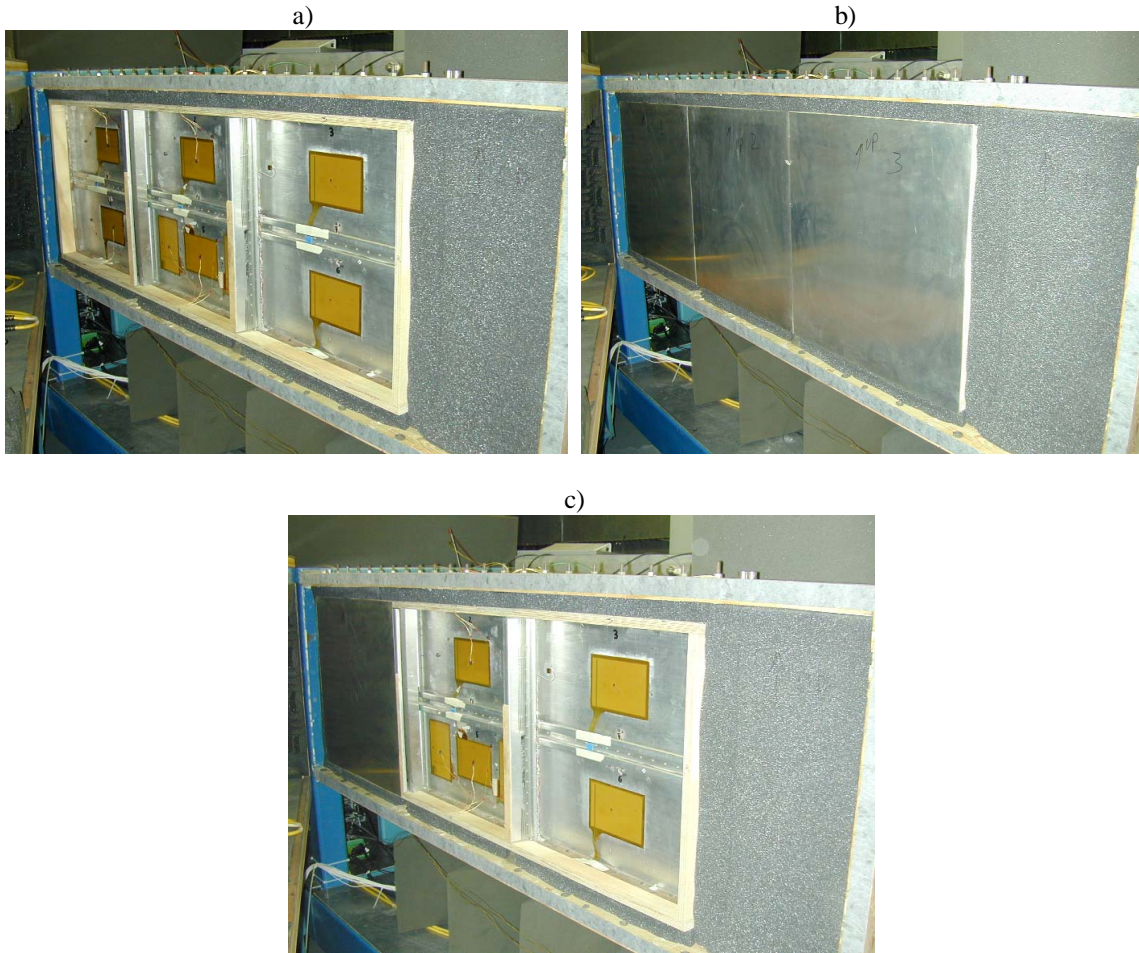


Figure 9: Trim panel configurations studied: a) all bays untreated, b) all bays treated, and d) bays 1 and 2 treated.

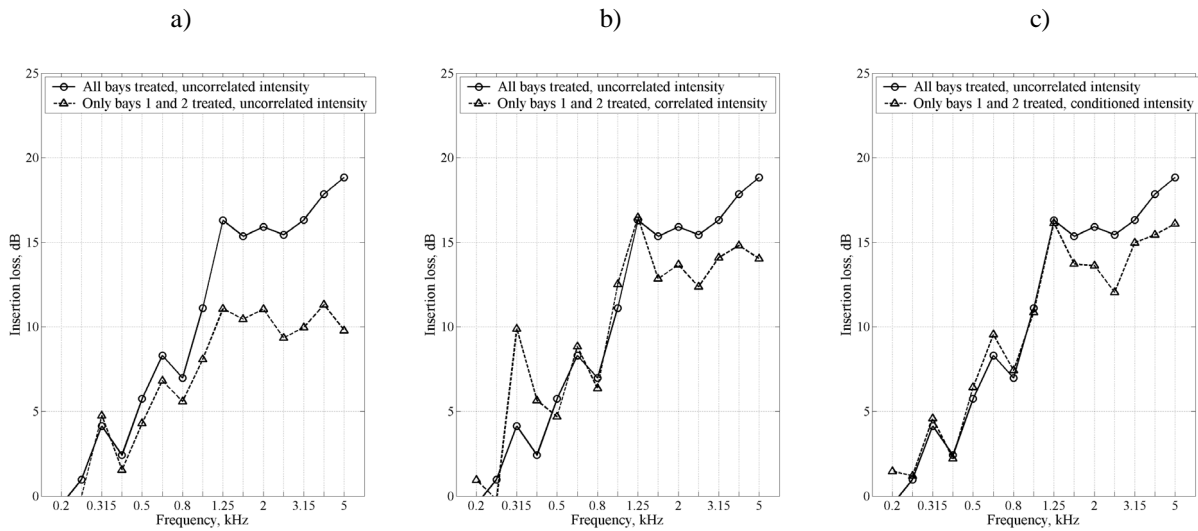


Figure 10: Comparison of insertion loss estimates: a) baseline insertion loss compared to uncorrelated insertion loss, b) baseline insertion loss compared to correlated insertion loss, and c) baseline insertion loss compared to conditioned insertion loss.